Case Studies in Chemical and Environmental Engineering 10 (2024) 100855

Contents lists available at ScienceDirect

Case Studies in Chemical and Environmental Engineering

journal homepage: www.sciencedirect.com/journal/case-studies-in-chemical-and-environmental-engineering

Case Report

Long-term performance evaluation of VCRS-based atmospheric water generation in arid climates

Batool Taher Khalaf [a], Nicolas Lopez Ferber [a], Mathieu Martins [b], Matteo Chiesa [a,c,*], Nicolas Calvet [a,d,1]

[a] Mechanical & Nuclear Engineering Department, Khalifa University, P.O. Box 127788, Abu Dhabi, United Arab Emirates
[b] Research Laboratories, Khalifa University, P.O. Box 127788, Abu Dhabi, United Arab Emirates
[c] Arctic Renewable Energy Center (ARC), Department of Physics and Technology, University of Tromsø, Tromsø, Norway
[d] Research and Innovation Center on CO_2 and Hydrogen (RICH), Khalifa University, P.O. Box 127788, Abu Dhabi, United Arab Emirates

ARTICLE INFO

Keywords:
Atmospheric water generation (AWG)
Specific energy consumption (SEC)
Coefficient of performance (COP)

ABSTRACT

The paper evaluates the EW-1000 Atmospheric Water Generation-Vapor Compression Refrigeration system (AWG-VCRS) as a sustainable alternative to seawater desalination in the GCC. Conducted in Masdar City, Abu Dhabi, from July 2023 to January 2024, the study measured temperature, humidity, energy consumption, and water production. Key findings include a peak water production of 1500 LPD in September and an average Specific Energy Consumption (SEC) of 0.26 kWh/L. Productivity decreased by 71 % in cooler, dryer months. With a coefficient of performance (COP) of 3.6, the system aligns with conventional air conditioners, highlighting its potential for enhancing water security in arid regions.

1. Introduction

Freshwater scarcity has become a significant global challenge in recent times, given its critical role in maintaining hygiene and safety, particularly in regions without access to surface or underground water reserves. With the expected rise in global temperatures and human needs, the demand for water is projected to increase by 55 % by 2050. Moreover, many countries face an issue of excessive water demand due to population growth and economic challenges [1].In addition, water stress in the Gulf Cooperation Council (GCC) countries is a pressing issue, as these nations often face the challenge of demand for water far exceeding the available natural resources. This region, characterized by its arid environment and scarce rainfall, heavily relies on non-renewable groundwater and costly desalination processes to meet its water needs. The situation is particularly acute in the United Arab Emirates (UAE), which ranks as the tenth most water-stressed country in the world. This high level of water stress indicates a critical reliance on nearly exhausted water supplies, raising concerns about sustainability and the urgent need for effective water management strategies. As the GCC countries continue to develop economically and demographically, the pressure on their water resources intensifies, making the implementation of innovative water conservation practices and technologies increasingly vital.[2] In the UAE, fresh groundwater levels have decreased over the past decade by 76 %, and water demand is expected to increase by 30 % in the next decade. The Water Resources and Integrated Management of UAE report of 2021 indicated that the increase in water demand is attributable to four primary contributors: agricultural, domestic, landscaping, and industrial water usage, as depicted in Fig. 1. Agricultural and domestic water use account for the majority of the rise in water demand due to the UAE's desire to cultivate its food rather than relying on imports, while the country's population is increasing drastically [2].

The UAE's three primary sources of water that supply the above-mentioned contributors are: 44 % of desalinated groundwater, 42 % of desalinated seawater, and 14 % of treated wastewater [3]. Due to its dry climate, limited surface water and lower annual precipitation compared to other countries, the UAE is primarily reliant on desalination processes for its freshwater supply. These sources of water introduce significant challenges, specifically in the desalination process. In the UAE, this process results in brine with salinity levels exceeding 40,000 mg/L in seawater desalination plants and higher than 10,000 mg/L in brackish

* Corresponding author. Arctic Renewable Energy Center (ARC), Department of Physics and Technology, University of Tromsø, Tromsø, Norway.
E-mail address: matteo.chiesa@ku.ac.ae (M. Chiesa).
[1] Current affiliation: Flexibility team, Energy Division, ENOWA/NEOM, NEOM, Saudi Arabia.
[2] W.Population, "Water Stress by Country 2024." [Online]. Available: https://worldpopulationreview.com/country-rankings/water-stress-by-country.

https://doi.org/10.1016/j.cscee.2024.100855
Received 11 June 2024; Received in revised form 12 July 2024; Accepted 13 July 2024
Available online 14 July 2024

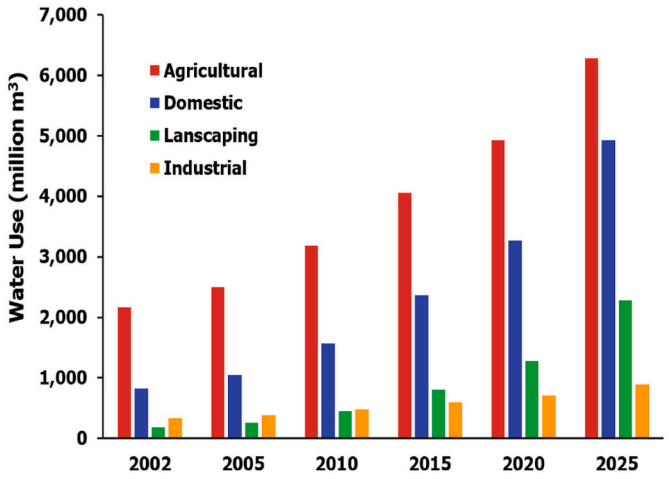

Fig. 1. Increasing water demand in the UAE [2].

groundwater desalination plants. The waste is discharged back into the environment, mainly the sea, and insufficient dilution can cause dead zones due to oxygen depletion, which can locally threaten marine life [4]. The salinity of the Gulf is becoming increasingly challenging, especially in the area of large desalination units along the shores of countries like the UAE, Qatar and Saudi Arabia within the GCC. These areas are witnessing a continuous rise in salinity due to the operations of these extensive desalination infrastructures. Moreover, centralized desalination plants require extensive pipelines to transport treated water to its intended destination, resulting in leakages and increased costs.[3] Furthermore, treated wastewater is being used in the UAE for non-drinkable purposes, such as irrigation of crops, landscaping, and industrial purposes, as the use of treated wastewater for drinking purposes is still limited in the UAE, due to concerns over public acceptance and potential health risks [5]. Research indicates that leafy greens absorb more heavy metals from wastewater irrigation than non-leafy plants. Nevertheless, small-scale farmers persist in cultivating these crops with untreated sewage to increase their income [6]. Furthermore, the financial and technical difficulties of processing wastewater at a central facility before sending it to dispersed agricultural and industrial areas in desert and coastal regions present another significant challenge [7]. Moreover, in GCC nations, the gap between water supply and agricultural demand is bridged by significant use of groundwater. This unchecked extraction has led to severe drops in groundwater levels, quality decline, saltwater encroachment into fresh aquifers, and increased pumping expenses. Such groundwater usage trends are unsustainable, necessitating urgent measures to limit extraction and preserve this crucial resource for both urban and rural water supplies [6]. The UAE's Water Security Strategy 2036 aims to address these issues by reducing the total demand for water resources by 21 %, lowering the water scarcity index by three degrees, and achieving a significant reduction in CO_2 emissions from the water desalination process.[4]

Atmospheric Water Generation (AWG) is seen as a viable method to supplement water supply, particularly useful in disaster relief, military operations, and remote areas where water transport costs are high [8]. AWG devices utilize dehumidification and condensation methods to extract water from airborne moisture, followed by filtration, UV sterilization, and re-mineralization, producing potable water [9]. Around 495,000 km^3 of water cycle through the atmosphere annually, with only 600 km^3 consumed.[5] AWG's advantage includes no brine waste production and adaptability to various settings, capable of generating various quantities of water daily. AWG techniques are split into passive (radiative cooling, sorption, fog harvesting) and active (thermoelectric cooling, condensate recovery, vapor compression refrigeration) systems. Passive systems harvest water through natural cooling and absorption processes, while active systems, like air conditioners and vapor compression refrigeration, condense air moisture. These systems vary in size and water production, affected by environmental factors such as humidity, temperature, and dust. The AWG-VCRS is ideal for the UAE due to its high humidity levels, low electricity costs, and strong technological infrastructure making it a cost-effective and sustainable solution for water generation [10].

In the context of AWG-VCRS, Essa Ansaris literature review [8] provides a detailed examination of their deployment across the Middle East. The review details a study in Dhahran, Saudi Arabia, where a small-scale AWG-VCRS system yielded 50.52 L/day over four months [11]. Furthermore, research conducted over a year in Bahrain across six cities revealed that small-scale AWGs produced 7.29–8 L/day, with Specific Energy Consumption (SEC) between 0.74 and 0.98 kWh/L. In Iraq, a small-scale AWG-VCRS system was assessed for its performance in August, managing to function within a 20%–80 % RH range and achieving a maximum water production of 13.11 L/day at a SEC of 1.068 kWh/L [12]. In the UAE, Sharjah's year-long study of an AWG device under varied climatic conditions recorded its highest water output in February at 29.8L, correlating with a temperature of 21.1 °C and 76 % RH. The lowest output was in January, at 0.13 L/hr., with SEC of 1.98 kWh/L, at 18.74 °C and 47.6 % RH. On an annual average, the device produced water at 0.36 L/hr., with SEC of 2.25 kWh/L, costing 0.18$/L [13]. Another study analyzed scalable AWG techniques using VCRS and Air Conditioner Condensate Recovery (ACCR) over four months in summer 2022 in Masdar City, Abu Dhabi, UAE. It evaluated the performance of three commercial VCRS-type AWG units, correlating their efficiency with the relative humidity and temperature of the inlet air in both indoor and outdoor settings. Additionally, the study captured up to 30.8 $L.day^{-1}.TR^{-1}$ from air conditioning condensates using a Fresh Air Handling Unit with a capacity of 7.87 $m^3\ s^{-1}$, installed atop a university building [8].

The available research on AWG highlights that current studies mainly focus on small-scale units, either over a year or shorter periods, revealing a gap in the long-term evaluation of large-scale AWG-VCRS systems. Addressing this, this research will investigate a large-scale AWG-VCRS in Abu Dhabi, UAE, for nine months using a commercially AWG-VCRS machine from Eshara Water (now Airwater Co.) company,[6] to assess its water production, specific energy consumption, and its efficiency under various climatic conditions, thereby providing a more comprehensive understanding of its performance and scalability.

2. Methodology

A commercially available AWG-VCRS system from Air Water Company (EW1000 machine) was assessed under various climatic conditions outdoors at Khalifa University Masdar Solar Institute Platform (KUMISP) in Masdar city, Abu Dhabi, UAE from July 2023 to march 2024 grasping seasons of summer and winter.

The Eshara Water (now Airwater Co.') EW1000 machine is an AWG-VCRS that has the capacity to generate 1000L/day of clean, cooled water using mineralization filters and UV treatment. The machine consists of

[3] "The Benefits of Decentralized Desalination," fluence news team. [Online]. Available: https://www.fluencecorp.com/benefits-of-decentralized-desalination/.

[4] UAE Government, "The UAE Water Security Strategy 2036," The UAE Water Security Strategy 2036. [Online]. Available:https://u.ae/en/about-the-uae/strategies-initiatives-and-awards/strategies-plans-and-visions/environment-and-energy/the-uae-water-security-strategy-2036.

[5] S. Graham, C. Parkinson, and M. Chahine, "The water cycle," NASA earth observatory. [Online]. Available: https://earthobservatory.nasa.gov/features/Water.

[6] "Air Water." [Online]. Available: https://airwaterco.com/.

two VCR systems, each including an air-cooled condenser, an axial-type condenser fan, a scroll compressor, an expansion valve, a finned-tube evaporator, and a centrifugal-type evaporator fan, along with centrifugal-type evaporator fans, and an air-to-air heat exchanger. The refrigerant loop uses the environmentally-friendly R417a fluid. The two VCR systems are independent of each other, ensuring continued operation even if one compressor fails. The machine operates by drawing in humid air from the top, which is then pre-cooled in the heat exchanger before entering the evaporators. The dry air is expelled through the condensers while the water is collected in trays and stored in the main tank. The system includes sensors at the inlet measuring the relative humidity and temperature, as well as sensors on the refrigerant line measuring the discharge and suction temperatures. In addition, there are pressure gauge sensors that can be recorded manually to find the saturation temperatures of the evaporator and condenser. During our evaluation, our primary goal was to achieve continuous water generation, which necessitated a strategic bypass of the main tank in the EW1000 system, as this tank is equipped with a level sensor to trigger the shutdown of the machine when full. Although essential for our objective, this modification led to the water bypassing the standard filtration process. For precise water production measurement, we integrated an external Monitoring Station (MS) into our setup. The modifications to the water extraction process are detailed in Fig. 2. It shows how water from the EW1000 is rerouted to a secondary tank, which is equipped with a level sensor. This sensor contains two floaters, spaced 12 L apart. When both floaters are immersed in water, it triggers a pump that then redirects the water to the KUMISP's main storage tank via the external MS. The EW1000 system's internal monitoring station (MS) is equipped with various sensors along the refrigerant and electrical lines. These sensors are strategically placed to monitor the system's performance and measure energy consumption accurately. In addition, the external MS includes extra sensors which measure the temperature and humidity of the ambient air and exhaust air.[7] The information gathered from these parameters is detailed in Table 1 offering an overview of the system's operational metrics.

For precise monitoring of ambient temperature, RH, and water generation (WG) rates, we utilized the data stored in the external MS. This approach enabled data to be collected at any time, with the MS recording at 5-min intervals. In parallel, the EW1000's refrigerant and electrical metrics were continuously captured via its data logger, set to connect to Wi-Fi. This configuration allowed for daily automatic transmission of data to Eshara Water (now Airwater Co.), captured in 10-min intervals, and subsequently formatted into text files. These files were then processed and transformed into Excel tables, enabling a detailed analysis of the system's performance across a range of parameters. In this data analysis, an hourly basis is chosen instead of instantaneous data analysis. This approach overlooks the potential 12-liter discrepancy due to the floaters' activation in the tank. It assumes that the errors from delayed pump activation, when the tank is full, are negligible over extended periods. This method prioritizes broader water flow trends over precise, moment-to-moment accuracy.

The daily and hourly WG rates of the system were analyzed in relation to various environmental and operational parameters, such as RH, ambient temperature, vapor content in dry air, and the temperature differential between the dew point and suction temperatures. This analysis was conducted to understand how these factors influence the system's performance in generating water and its SEC. Additionally, a box-and-whisker plot is utilized to analyze the variations in WG across different hours. This type of plot provides a clear visual representation of the data's distribution, highlighting the median, quartiles, and any potential outliers, thus offering a comprehensive overview of the temporal fluctuations in WG. Furthermore, the Coefficient Of Performance (COP) of the system was measured to evaluate its efficiency. By examining the relationship between these variables and the system's output, the research aims to provide a detailed characterization of the system's behavior under different conditions.

3. Experimental results and discussion

The results obtained after evaluating the VCRS-AWG under Abu Dhabi's climatic conditions are showcased in this section. The evaluation period extended from July 2023 to March 2024, with the results systematically divided into summer and winter sections to reflect the system's seasonal performance. Additionally, a section on thermodynamic analysis is included, focusing on measuring the system's efficiency. The supplementary data indicates that System 1 was non-operational, resulting in WG rates that were approximately half of the expected output. The restoration of System 1 in September allowed both systems to reach full operational capacity, enhancing the WG rates. This supplementary document provides WG rates, along with corresponding relative humidity (RH) and temperature, and energy consumption from July 2023 to March 2024.

3.1. Summer results

Data regarding daily WG, ambient RH, and temperature were systematically collected and extracted from the external MS, and later analyzed using Python. In the initial months of July and August, System 1 was non-operational, leading to WG rates approximately half of the anticipated output. The restoration of System 1 in September enabled full operational capacity for both systems, resulting in improved WG rates. In July, the machine averaged 462 L/day, increasing to 464 L.day^{-1} in August, followed by a significant rise to 1112 L.day^{-1} in September and 1174 L/day in October. A notable peak in WG of 927 L was recorded in a single day of August, with only one system operational at RH of 81 % at night. This trend continued with increased productivity in the following months: a maximum WG of 1496 L in September and 1470 L in October, evidencing enhanced performance with both systems functioning, with production often exceeding the rated capacity. Additionally, the average hourly water production for these months is illustrated in Fig. 3. The primary axis displays water production values, while relative humidity and temperature values are plotted on the secondary axis. These plots demonstrate a distinct pattern in water production: higher output at night attributed to increased RH and cooler temperatures, and lower production during the day corresponding with decreased RH. This pattern highlights a direct correlation between water production levels and the interplay of temperature and RH values. While the levels of WG have shown a clear relationship with relative humidity, indicating how close the air is to saturation, it's also important to consider the mixing ratios for a more absolute perspective. Mixing ratio measures the mass of water vapor in a unit of dry air, represented in grams per kilogram. In September, mixing ratios at the inlet (w_{in}) was determined using Eq. (1) [14]. This analysis highlighted a trend shown in Fig. 4 during midday, the atmosphere exhibits low moisture content. This condition, marked by reduced mixing ratios, leads to decreased efficiency in AWGs for condensing water. Conversely, nighttime and early morning periods show increased moisture content, creating ideal conditions for AWGs to effectively condense water. At noon, when the moisture content is low, conditions become ideal for dehumidification processes in dehumidifiers, on the other hand, for AWGs, these periods of low atmospheric moisture represent the least efficient times for water condensation.

$$w_{in}\left[\frac{kg}{kg}\right] = \frac{0.622 \times P_v}{P_{atm} - P_v} \quad (1)$$

[7] After failure of the sensors located at the exhaust, these were later replaced by another set of probes, independent from the external MS.

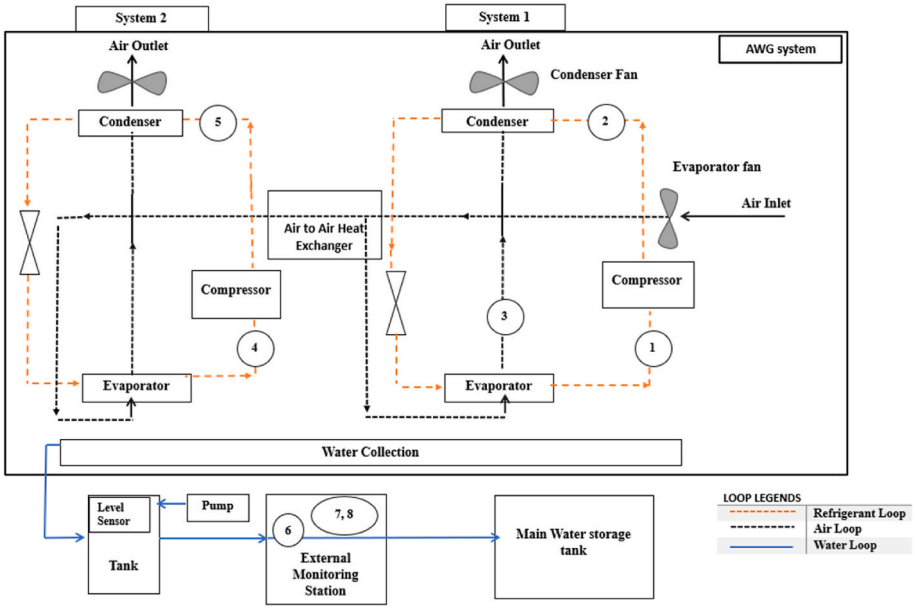

Fig. 2. Experimental setup for EW1000.

Table 1
Sensor parameters for the EW1000 Machine setup.

MS	Number	Parameter
Internal MS	1	System 1: Suction Line Temperature ($^{\circ}C$)
	2	System 1: Discharge Temperature ($^{\circ}C$)
	3	Air Temperature after evaporation ($^{\circ}C$)
	4	System 2: Suction Line Temperature ($^{\circ}C$)
	5	System 2: Discharge Temperature ($^{\circ}C$)
External MS	6	Water Generation (L)
	7	Ambient Temperature ($^{\circ}C$)
	8	Ambient Relative Humidity (%)

$$P_v\ [Pa] = 610.728 \times e^{\left(\frac{17.578 \times T_{a.in}}{242.45 + T_{a.in}}\right)} \times \left(\frac{RH_{in}}{100}\right) \quad 2$$

P_v is the partial pressure of water vapor in air [Pa], $T_{a,in}$ is the inlet ambient temperature in [$^{\circ}C$], RH_{in} is the inlet ambient relative humidity in [%].

The evaporator unit of the VCRS-AWG functions to cool the air below its dew point, thereby facilitating the condensation process. To illustrate the evaporator's condensation capability, a temperature differential is considered, ΔT (defined as the difference between the dew point temperature, T_{dp}, and the suction line temperature, $T_{suction}$), dew point temperature can be measured using Eq. (3) and Eq. (4) [15]. This differential $\Delta T = T_{dp}\text{-}T_{suction}$, is a critical measure of the system's effectiveness in facilitating condensation. During peak daytime hours, particularly around noon, there is a notable increase in ambient temperatures, which often leads to a higher $T_{suction}$. Consequently, during these periods, a smaller ΔT is observed. This smaller ΔT indicates that while the system still cools the air below its dew point, it does so by a lesser margin than during cooler times of the day. This limitation in cooling efficiency translates into less effective condensation, thereby reducing WG rates. Conversely, the nighttime and early morning hours are characterized by cooler ambient conditions, resulting in a lower $T_{suction}$. These periods experience an increase in the differential ΔT, accompanied by an increase in RH. A larger ΔT increases the rate of heat transfer, therefore improving the condensation of moisture from the air, which leads to increased WG, as shown in Fig. 5.

$$\gamma(T, RH) = 17.27\left(\frac{T_{a.in}}{237.7 + T_{a.in}}\right) + Ln\left(\frac{RH_{in}}{100}\right) \quad 3$$

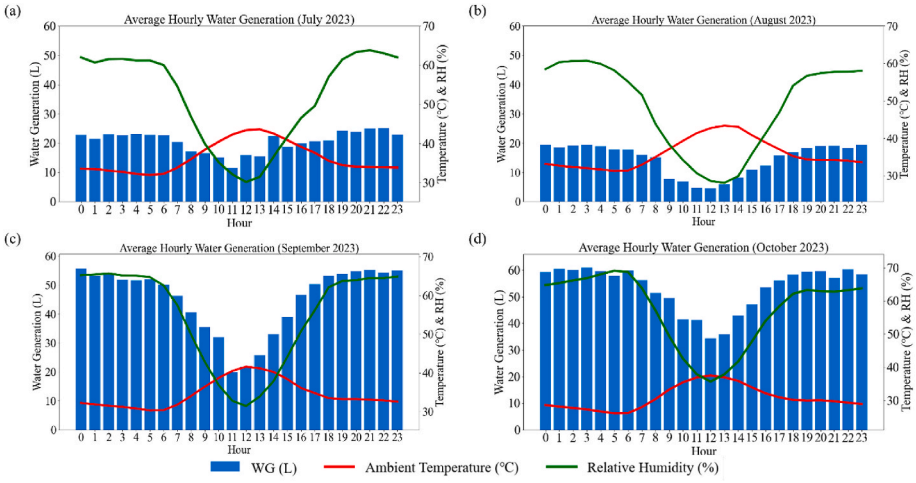

Fig. 3. Average hourly Water generation against Ambient Temperature and Relative Humidity in (a) July, (b) August, (c) September and (d) October of 2023.

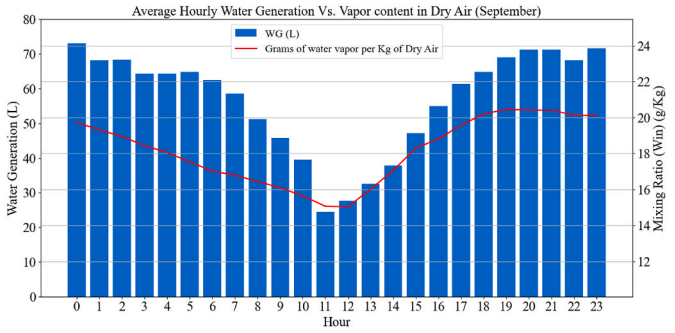

Fig. 4. Average hourly water generation against average hourly mixing ratios at the inlet.

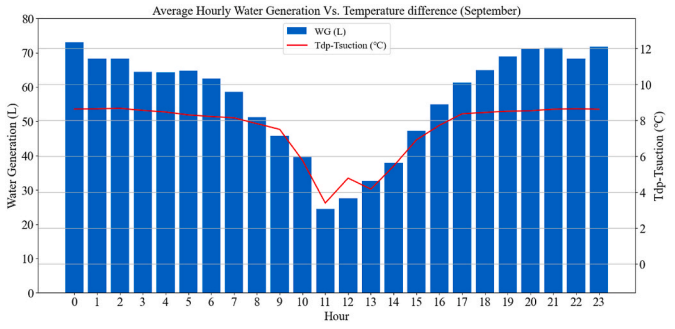

Fig. 5. Average hourly Water generation against the difference between dew point and suction line temperature in September.

$$T_{dp} = \frac{(237.7 \times \gamma(T, RH))}{(17.27 - \gamma(T, RH))} \quad 4$$

In a box and whisker plot; the first quartile (Q1) identifies the threshold below which 25 % of the dataset falls, essentially serving as the median of the dataset's lower half. Conversely, the third quartile (Q3) acts as the median of the dataset's upper half, marking the point beneath which 75 % of the data is found. The dispersion of the central 50 % of the data is measured by the Interquartile Range (IQR), calculated as the difference between Q3 and Q1. In addition, the IQR is indicative of data variability; a more compact box suggests less fluctuation in the WG rates, thereby denoting a greater consistency in the average WG. The lower and upper whiskers denote the dataset's minimum and maximum values within the non-outlier range. The upper whisker is determined as the maximum data point that is less than Q3+1.5 × IQR, establishing the upper boundary for non-outlier data. Similarly, the lower limit is derived from Q1-1.5 × IQR; if the dataset's minimum value exceeds this lower limit, it is then considered the plot's minimum value [16]. Data points lying outside the bounds set by the upper and lower limits are considered as outliers represented as dots [17]. Median values have been excluded from the graphs to specifically highlight the average hourly WG. In Fig. 6, the plotted data for September and October reveal some patterns. During nighttime and early morning hours, the boxes appear narrower, indicating less variability in WG rates. This observation is consistent with more stable conditions during these times. However, at noon, the boxes are observed to be wider, reflecting a greater variability in WG rates, it suggests that the variations are influenced by changes in RH and temperature. The instance of the minimum whisker reaching zero during midday hours agrees with the maintenance periods when the inlet filters of the machine were cleaned, and the machine was temporarily shut down, thereby affecting WG rates. The outliers above the upper whisker in the graph indicate that during certain hours of the day, the RH was exceptionally high, surpassing the typical range for the month. Conversely,

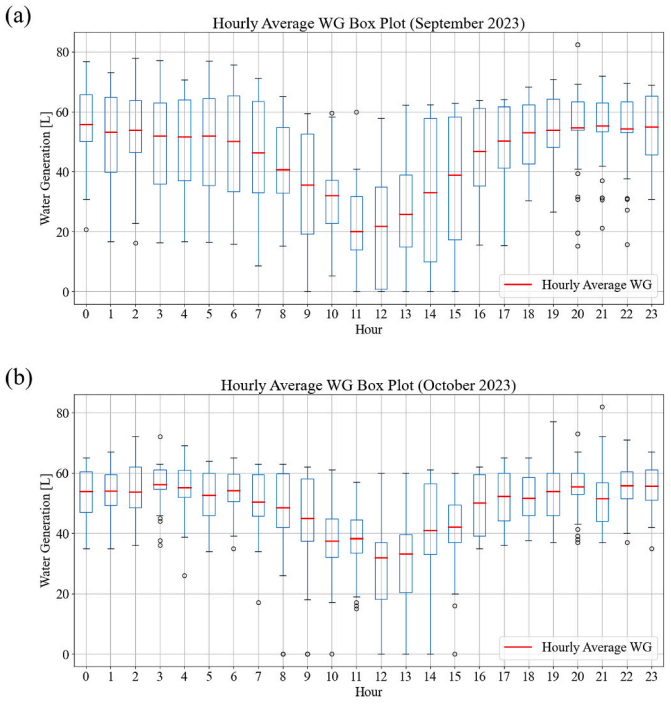

Fig. 6. Box and Whisker plot with the average hourly WG in (a) September and (b) October.

the outliers below the lower whisker suggest that on some days, WG levels were lower due to decreased RH levels. The variations in the widths of the boxes between September and October are attributable to the operational period of one subunit VCRS system for five days in September, which resulted in a broader range due to increased variation. This statistical analysis offers a comprehensive understanding of how variations in RH and Temperature directly impact the consistency of WG levels.

The average hourly SEC represented in Eq. (5), documented for the months of July, August, September, and October, as shown in Fig. 7. The machine's energy consumption was tracked from the internal MS, while WG data was sourced from the external MS. Due to differing data frequencies between the two Monitoring systems, Python was utilized to interpolate the datasets, ensuring uniform hourly data points for analysis. In calculating the SEC, it was observed that several data points significantly exceeded the typical range observed in the rest of the SEC dataset. These data points were identified as outliers, largely attributable to periods when WG approached zero. Consequently, for WG levels ranging from 0 to 3 L, the data were considered non-representative and

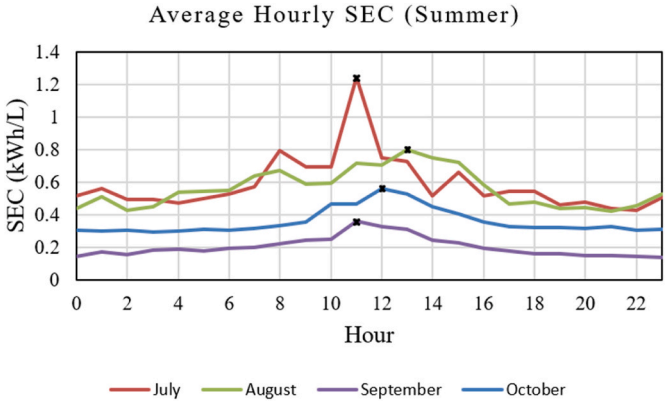

Fig. 7. Average hourly Specific Energy consumption in summer season, the stars represent the maximum SEC per month.

thus excluded from the analysis. The SEC decreases at night due to the lower temperature of the incoming air, which requires less energy to be cooled below the dew point temperature. SEC was maximum at 1.24 kWh/L, 0.8 kWh/L, 0.35 kWh/L, and 0.56 kWh/L from July to October respectively. The uneven graph for August's SEC is attributed to the limited availability of energy consumption data for that month. The scarcity of data points might have led to a lower, potentially approximate SEC value, which may not fully represent August's SEC. The average hourly SEC in July recorded 0.6 kWh/L, 0.56 kWh/L in August, 0.26 kWh/L in September, and 0.36 kWh/L in October. In September and October, SEC dropped significantly when both systems operated simultaneously compared to July, when only one system was functional. This improvement in SEC can be attributed to the energy usage dynamics when System 1 was inactive. Although System 1 was not producing water, its condenser and evaporator fans remained active, consuming energy. This scenario represents inefficiency, as the energy consumed by the fans did not contribute to the system's primary function of WG. Consequently, the energy used by the fans, in the absence of water production from System 1, was not effectively converted into the desired output, resulting in an elevated SEC. In contrast, when both systems were active and generating water, the energy consumed by the fans was utilized more productively. This efficiency stems from the fact that the energy, including that used by the fans, contributed to water production in both systems, leading to an improved energy-to-water production ratio and thus decreasing the SEC.

$$\mathrm{SEC}\left[\frac{\mathrm{kWh}}{\mathrm{L}}\right]=\frac{E}{m_w} \quad (5)$$

Where E is the energy measured from the internal MS of the system in [kWh], and m_w is the collected water in [L].

3.2. Winter results

During the winter months spanning November 2023 to March 2024, the performance of the AWG declined from November to February due to reduced RH and cooler temperatures, with a noticeable improvement beginning in March. In December, frost began to accumulate around the compressors due to the drop in ambient temperatures, leading to the evaporator cooling below the dew point significantly. This, combined with minimal heat absorption by the evaporator, resulted in the coils becoming increasingly colder over time, allowing any condensation on the coils to freeze and form frost. To address this issue, a threshold temperature of 23 °C was set. When temperatures fell below this point, the system would automatically shut down to prevent further cooling and thus avoid additional frost formation. Consequently, in December and January, the AWG was inactive for most hours of the day due to the low ambient temperatures, which significantly reduced the production of water. The average daily WG rates were observed to be 836.2 L.day^{-1} in November, 474 L.day^{-1} in December, 366 L.day^{-1} in January, 287 L.day^{-1} in February, and 538 L.day^{-1} in March. WG rates in November dropped by 33 % compared to those in September, the peak summer month The average hourly WG for the months from December 2023 to March 2024 is shown in Fig. 10. The WG trend in December and January deviated from expected performance patterns of AWGs. The machine generated more water at lower RH levels around noon, related to a threshold temperature setting initiated in December. The machine activates when ambient temperatures exceed 23 °C, which occurs around midday. Therefore, average hourly WG rates were higher at the time of elevated temperatures and reduced RH levels. In January, WG rates fell by 71 %, followed by a further 74 % drop in February, and a 52 % decrease compared to September, marking winter as the least efficient season for water production by the AWG. However, in March, rates began to rebound, reaching approximately half of the expected levels.

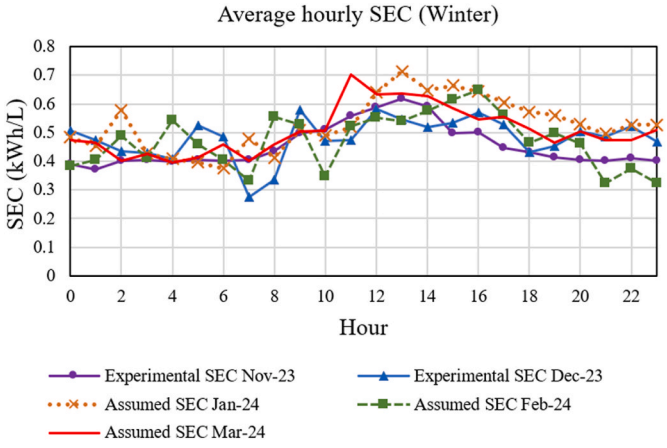

Fig. 9. Average hourly SEC from November 2023 to March 2024, showing experimental SEC data for November and December, and estimated SEC values for January to March due to logger malfunction.

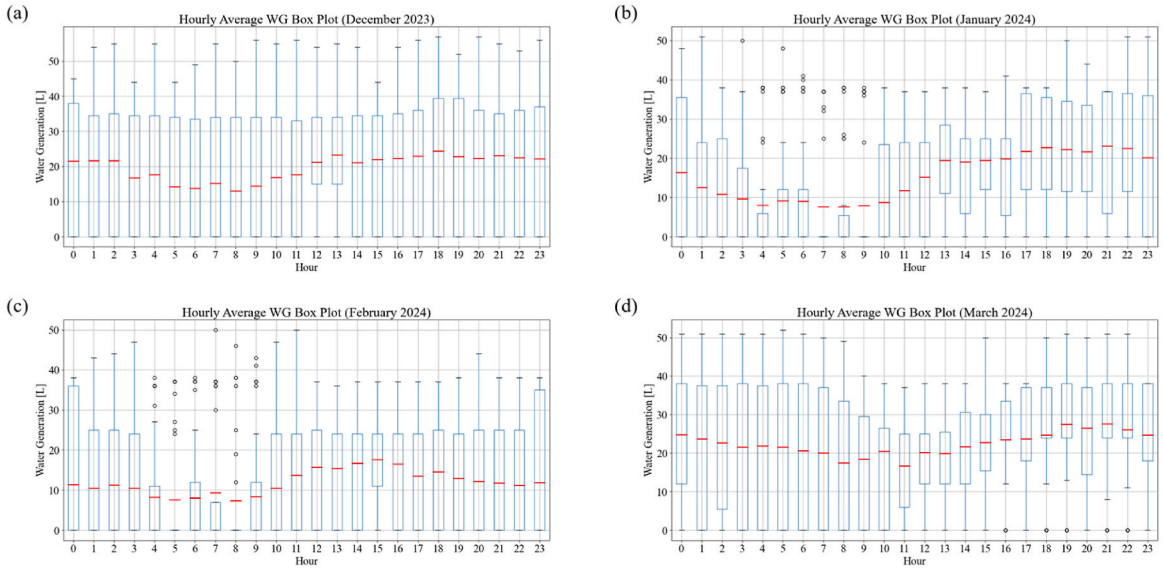

Fig. 8. Hourly Average water generation Box and Whisker plot for (a) December 2023, (b) January 2024, (c) February 2024, and (d) March 2024.

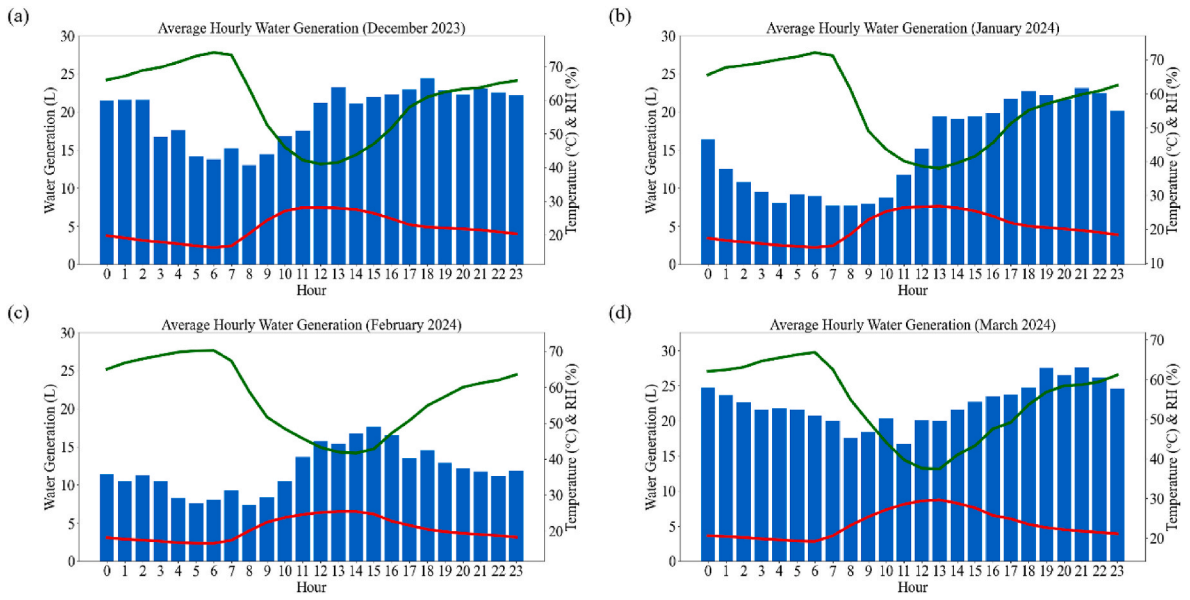

Fig. 10. Average hourly Water generation in (a) December 2023, (b) January 2024, (c) February 2024 and (d) March 2024.

This uptick indicates that from March onward, rising ambient temperatures and relative humidity are beginning to enhance production rates.

The box plot in Fig. 8a illustrates the average hourly WG for December, revealing that the lower whisker for each hour extends to zero. This indicates that there were instances each hour when the machine was either inactive or failed to produce any water. Most hours exhibit significant variation, except for 12 p.m. and 1 p.m., which display the smallest range of variation. This consistency suggests that during these midday hours, the machine remained operational due to ambient temperatures surpassing the threshold temperature. The extended upper whiskers demonstrate that on days with high relative humidity, the machine produced significant amounts of water. For January, as depicted in Fig. 8b–a notable pattern emerges at 4 a.m., where the average WG closely approaches the upper whisker. Despite numerous zero readings, a sufficient number of higher WG instances elevated the average to near the upper limit. At 7 a.m. and 8 a.m., the box plot becomes nearly invisible due to over half of the data points registering as zero, thus compressing the visual representation of the box. During these hours, no upper whiskers are visible because the maximum values were outliers, exceeding the threshold of Q3 + 1.5*IQR. On certain days, the hours between 4 a.m. and 9 a.m. experienced higher relative humidity and temperatures than the same timeframe on other days, causing the WG rates to be considered outliers and falling outside the typical range. In February (Fig. 8c), at 5 a.m. and 8 a.m., inactivity during these hours resulted in the plots compressing to zero. In contrast, March (Fig. 8d) showed fewer outliers and more consistent WG rates towards noon and nighttime, indicating enhanced ambient conditions favorable for the machine's operation.

The average hourly SEC from November 2023 to March 2024 is depicted in Fig. 9 In January, the internal logger that tracks energy consumption malfunctioned, leading to missing data after January 19th. Consequently, the energy data for the subsequent 10 days were extrapolated based on the preceding 20 days. The difference in temperature between the inlet and outlet ambient temperatures indicates the machine's operational status: a significant difference suggests full operation at 14 kW, no difference indicates a shutdown with zero energy consumption, and intermediate differences point to varying levels of energy use. From January 19th onward, the SEC was estimated. The outlet sensor from Elitech GSP-6 model has been installed late December at the condenser's outlet to measure both the temperature and RH.[8]

The SEC data for the winter months, specifically from December to February, exhibit an irregular trend primarily due to periods when the machine was inactive or failed to produce water, leading to sparse data points. In February, the SEC dropped to an average of 0.47 kWh/L, largely because the machine was frequently inactive due to the lowest temperatures of the season. Starting in March, as ambient temperatures and relative humidity began to rise, the SEC curve smoothed out, averaging 0.50 kWh/L. This improvement is expected to continue, with a decrease in SEC due to enhanced energy-to-water ratios as conditions become more favorable. The average SEC values over these months were 0.45 kWh/L in November, 0.48 kWh/L in December, 0.53 kWh/L in January, 0.47 kWh/L in February, and 0.50 kWh/L in March.

3.3. Thermodynamic results

A typical VCR system is composed of four components: comprising of a compressor, condenser, an expansion valve, and an evaporator. In this context, temperature and pressure readings in the refrigerant line shall be taken at different points in the system to enable a thermodynamic assessment. These values are crucial since they offer essential information about the enthalpies of each point. In assessing the EW1000, temperature measurements are taken from both the suction and discharge locations, while pressure readings are manually recorded using pressure gauges on these lines. As illustrated in Fig. 11, the refrigeration cycle begins with saturated vapor entering the compressor, where it is compressed and leaves as superheated vapor. Following this, the refrigerant exits the condenser as saturated liquid, then enters the evaporator as a mixture of vapor and liquid from an expansion valve.

The COP was calculated by interpolating enthalpy for R417a values from thermodynamic tables, aligning them with the system's suction and discharge temperatures. The COP, as derived from Eq. (6) [18], represents the ratio of cooling capacity to the compressor's work. Since the refrigerant's mass flow rate was not provided, Eq. (7) was employed to define the energy transfer process from the air to the refrigerant in the evaporator, necessitating the air's mass flow rate [19].

The volumetric flow rate of air was determined using an anemometer

[8] "Elitech Technology, Inc." [Online]. Available: https://www.elitechus.com/.

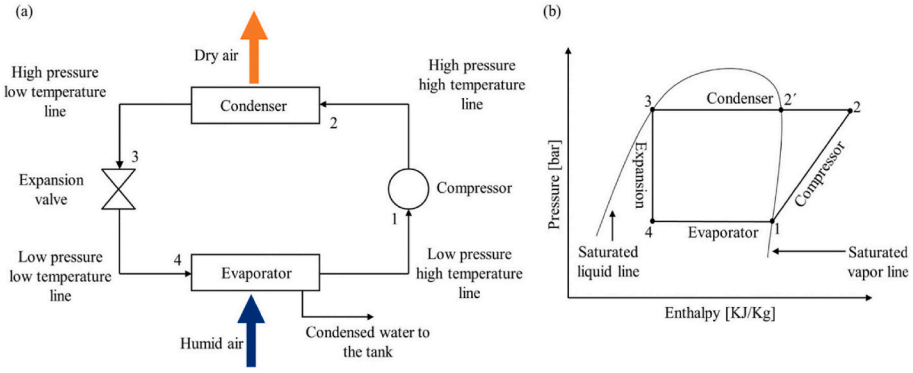

Fig. 11. (a) Components of VCRS, (b) P-h diagram of ideal VCRS [10].

to measure the inlet velocity of 1.6 m/s across an inlet area of 0.65 m^2, yielding a flow rate of 3762 m^3/hr. To validate this value, Eq. (8) was utilized to ascertain theoretical WG rates, which were then compared to experimental WG rates. The comparison revealed a marginal 7 % difference shown in Fig. 12, corroborating the reliability of the flow rate assumption for thermodynamic analysis. Subsequently, with the air flow rate established, Eq. (7) facilitated the determination of the refrigerant's mass flow rate. Given the compressor's work input of 5.2 kW (10.4 kW accounting two compressors), the COP was calculated to be 3.6. This efficiency level is within the standard range for air conditioning units, suggesting that enhancements designed to elevate COP in air conditioning technology could also be beneficial for AWG units, implying that methods aimed at improving the COP in air conditioning systems might prove equally advantageous for AWG units.

$$\mathrm{COP}\left[\frac{\mathrm{kJ/hr}}{\mathrm{kJ/hr}}\right]=\frac{\mathrm{Q_{evap}}}{\mathrm{W_{comp}}}=\frac{\dot{m}_{\mathrm{ref}}\,(h_1-h_4)}{10.4\ \mathrm{kW}\times 3600} \tag{6}$$

$$\dot{m}_{\mathrm{ref}}\left(h_{\mathrm{out,evap}}-h_{\mathrm{in,evap}}\right)=\dot{m}_{\mathrm{air}}\left(h_{\mathrm{out,air}}-h_{\mathrm{in,air}}\right) \tag{7}$$

$$\dot{m}_w\left[\frac{kg}{hr}\right]=m_{air}(w_{in}-w_{out}) \tag{8}$$

4. Discussion

AWGs are not limited to their water production capabilities but can also offer complementary benefits, enhancing their applicability across various settings. These machines can serve as a substitute or complement to traditional heating (through condenser or hot air exhaust heat recovery), ventilation, and air conditioning (HVAC) systems, thereby offering a cooling/heating solution that simultaneously produces water. Additionally, their dry air exhaust can be of used in applications such as drying. The ability of AWGs to deliver these additional products can significantly enhances their usability and value, presenting them as a versatile solution in both every day and specialized applications. Real-world testing in Dubai [20], demonstrated that an integrated AWG system could supply the daily drinking needs of 792 people while saving over 11 tons of plastic waste per year (replacing drinking water bottles). The machine's heating capabilities were also substantial, providing hot water for two buildings housing 200 guests each and meeting 70 % of the heating requirements for one of the kitchen buildings. Additionally, the cooled and dry air produced by the AWG covered 87 % of the fresh air needed for common kitchen areas. This multifaceted functionality underscores the practical benefits and environmental impact of deploying AWG technology in urban settings.

In the UAE, managing surplus solar power during peak sunlight hours is a complex challenge, particularly at large-scale solar installations such as Al Dhafra Solar PV, Sweihan Solar PV Park, and Mohammed bin Rashid Al Maktoum Solar Park. During these hours, the energy production can exceed demand or grid intake capacity, leading to the need for curtailment, where excess power is intentionally not generated to avoid overloading the grid. This curtailment increases the Levelized Cost of Electricity, as the potential output of the solar plants isn't fully utilized. To address this inefficiency, the integration of innovative systems like AWG-VCRS presents a compelling solution. These systems are particularly energy-intensive, making them ideal candidates for using surplus electricity that would otherwise be curtailed. Although water productivity through AWG during midday is decreased due to lower humidity levels, it adds value to the otherwise wasted solar electricity. This strategy turns a potential economic loss into a productive outcome by generating a valuable resource—cold, low-mineralized water suitable for various purposes. This water can be

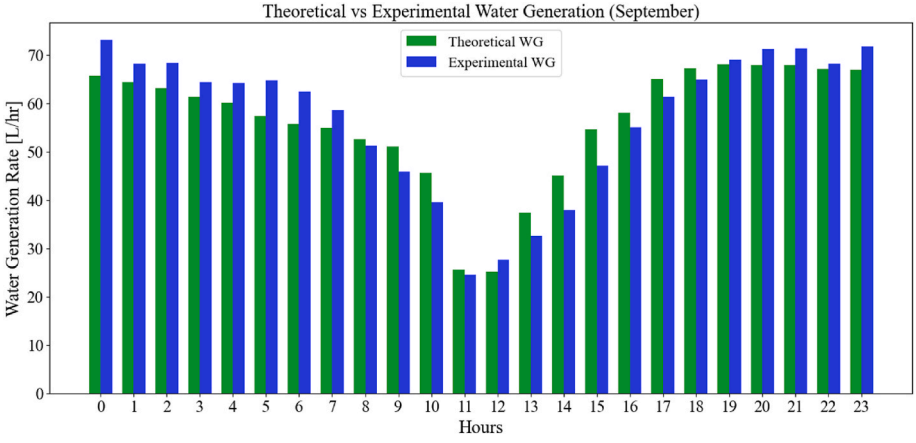

Fig. 12. Theoretical WG Vs Experimental WG for volumetric flow rate validation.

used strategically to maintain the solar panels themselves, as dust accumulation and heat can significantly reduce solar panel efficiency, and regular cleaning with the produced water can help maintain optimal performance. This not only ensures the solar installations operate efficiently but also provides a sustainable use for excess electricity. While the high energy consumption of AWG-VCRS systems is a notable drawback, evaluating the sustainability of this approach should go beyond the simple metric of energy needed per liter of water produced. It's essential to consider the broader benefits, such as enhancing solar power system efficiency and contributing to water resource management in a region where water scarcity is a pressing concern. This holistic view of sustainability could justify the initial high energy investment by aligning it with long-term environmental and economic gains for the UAE.

To fully understand and optimize the deployment of AWGs, a comprehensive evaluation encompassing Life Cycle Assessment (LCA), techno-economic analysis, and system analysis, including grid services, is essential. The LCA would provide insights into the environmental impacts throughout the device's lifespan, from production to disposal, while the techno-economic analysis would assess the financial feasibility and operational efficiencies of these systems. Additionally, system analysis would explore how these AWGs could integrate with and benefit the existing power grid, potentially offering services such as load balancing and demand response. Such detailed examinations would greatly enhance the research and development community's knowledge of these devices, uncovering valuable use cases and identifying potential areas for improvement in their application within renewable energy systems.

Previous experimental studies on AWG-VCRS systems are scarce and typically limited to short time periods, small-scale setups, or lab environments. One notable exception is a long-term evaluation of a small-scale AWG-VCRS over one year. Our study, conducted over nine months, evaluated a large-scale device under the harshest weather conditions of both summer and winter. The comparison of average environmental conditions, water production, and energy consumption is presented in Table 2. Moreover, while previous studies tested only single VCR systems, our study employs two VCR sub-units. This dual sub-unit configuration addresses potential complications and enhances system reliability by providing redundancy. If one sub-unit fails, the other can continue operating, ensuring continuous water production. Additionally, the two sub-units allow for better management of cooling and heating cycles, leading to higher overall system efficiency and improved SEC. As shown in Table 2, our study achieved the lowest SEC range.

5. Conclusion

The Gulf region's arid climate leads to significant water scarcity challenges. Currently, desalination and the use of treated wastewater address this issue, yet these methods are energy-intensive and environmentally harmful, in addition to being reliant on centralized infrastructures. In response to the ongoing need for water and to reduce marine pollution, the deployment of AWG system in the GCC countries could enhance existing water production methods. These AWG systems, which extract moisture from the air, offer a more sustainable and decentralized alternative to traditional water supply technologies. AWG do not require liquid water and can be used anywhere where electricity is available opposing to RO, desalination, which requires a constant water supply. A large-scale commercial AWG unit, the EW1000, was evaluated outdoors over 8 months period., showing that SEC fluctuated, peaking at noon due to low relative humidity and high temperature. During summer (July to August of 2023), with one VCR system operational, it averaged 467 L/day of water production at 0.58 kWh/L SEC. With two VCR systems (September to October 2023), production increased to 1143 L/day, reducing SEC to 0.31 kWh/L. In winter (November 2023 to March 2024), the AWG produced 500 L/day with an SEC of 0.49 kWh/L, February was the least efficient month in Winter for water production, with production rates dropping by 75 % compared to September. The COP for the VCR-AWG system was 3.6, aligning with the COP of air conditioning systems.

The present study highlights a remarkable SEC compared to other VCRS-AWG systems. However, the very high energy requirements, especially when compared to typical water treatment systems like Reverse Osmosis (RO) which require about 0.005 kWh/l [27], cannot be overlooked. The viability and industrial potential of such a system will therefore be conditioned by factors such as the critical unavailability of surface water -including wastewater that could be treated by conventional water treatment systems and reused-, unreliability of conventional water distribution systems, whether due to acute failures from natural disasters or incidental causes, or structural issues like under-capacity, remote locations, and aging infrastructures. Additionally, the high availability of low-cost electricity from sources like photovoltaics, wind, or excess grid electricity, and the potential for offtakers for the AWG-VCRS byproducts (such as heat at the condenser and dry air at the exhaust) to provide additional value for domestic hot water or drying applications, will also play crucial roles. The significant variability in both SEC and productivity presents a reliability issue for AWG systems. Therefore, interesting pathways for improvement could include implementing control strategies to keep SEC within a predefined acceptable range, combining the AWG device with another upstream system to stabilize temperature and humidity at the intake, allowing the

Table 2
Comparison with existing literature on experimental AWG-VCR systems.

Rated capacity [L.day^{-1}]	Evaluation period	Evaluation conditions	Productivity [L.day^{-1}]	SEC [kWh/L]	Reference
20	6 months	T: 20 – 36°C RH: 50–71 %	8.18 ± 0.66 9.7 ± 1 9 ± 1 7.85 ± 0.5 7.3 ± 0.5 5.74 ± 0.8	0.88 0.74 0.8 0.92 0.99 1.25	[21]
NA	8 months	T: 35°C RH:95 %	42.72	0.75	[22]
30	4 months	T: 25 – 50°C RH: 20–80 %	23.6	1.13	[23]
12–16	1 month	T: 20 – 35°C RH: 20–80 %	7.29–8	0.74–0.98	[24]
32	1 year	T: 20 – 40°C RH: 20–65 %	3.12–22.8	0.63–0.99	[25]
NA	NA	T: 1 7 – 40°C RH: 27–95 %	6.72–43	0.75–4.71	[26]
1000	**9 months, outdoors**	**T: 25–50°C RH: 20–95 %**	**400–1200**	**0.3–0.6**	**This study**

device to operate at peak efficiency (such as through water vapor separation from the airstream or connection to a consistently moist exhaust), and increasing the quality and operation of components to enhance the system's COP, in line with ongoing engineering efforts in the air-conditioning industry, such as variable speed compressors, innovative refrigerant fluids, and heat exchange coil improvements.

CRediT authorship contribution statement

Batool Taher Khalaf: Writing – original draft, Visualization, Methodology, Investigation. **Nicolas Lopez Ferber:** Writing – review & editing, Supervision, Methodology, Conceptualization. **Mathieu Martins:** Supervision, Resources, Project administration. **Matteo Chiesa:** Writing – review & editing, Supervision, Project administration. **Nicolas Calvet:** Supervision, Project administration, Funding acquisition, Conceptualization.

Declaration of competing interest

The authors declare that they have no known competing financial interests or personal relationships that could have appeared to influence the work reported in this paper.

Data availability

Data will be made available on request.

Acknowledgements

This research is supported by ASPIRE, the technology program management pillar of Abu Dhabi's Advanced Technology Research Council (ATRC), via the ASPIRE VRI (Virtual Research Institute) Award No. VRI20-07.

The AWG device was provided as an in-kind by Eshara Water (now Airwater Co.), and the project benefitted from the work of their support team, most notably Eng. Arun Steephan. The authors also acknowledge the contribution of KUMISP staff Eng. Hanif Shaif, notably the machine's maintenance operations.

References

[1] V. Marchal, et al., "OECD environmental Outlook to 2050 Chapter 3: climate change," no. November, in: OECD Environmental Outlook, OECD, 2011, p. 90, https://doi.org/10.1787/9789264122246-en.

[2] A.S. Alsharhan, Z.E. Rizk, Overview on global water resources, in: Water Resources and Integrated Management of the United Arab Emirates vol. 3, Springer International Publishing, 2020, pp. 17–61, https://doi.org/10.1007/978-3-030-31684-6_2. World Water Resources, vol. 3. , Cham.

[3] M. Ahmed, S. Al, The Soft-Path approach for sustainable water management : an analysis of its Suitability in Abu Dhabi. https://scholarworks.uaeu.ac.ae/poli_sci_theses/5, 2018.

[4] M. Ahmed, W.H. Shayyab, D. Hoey, J. Al-handaly, Brine disposal from reverse osmosis desalination plants in Oman and the United Arab Emirates, Desalination 133 (2001) 135–147.

[5] T. Chfadi, M. Gheblawi, R. Thaha, Public acceptance of wastewater reuse: New evidence from factor and regression analyses, Water (Switzerland) 13 (10) (May 2021), https://doi.org/10.3390/w13101391.

[6] A.S. Qureshi, Challenges and Prospects of using treated wastewater to manage water scarcity Crises in the, Water J. 12 (1971) (2020) 1–16, https://doi.org/10.3390/w12071971.

[7] I. Abd, E. Alban, K. Abeer, E. Shahawy, Environmental rethinking of wastewater drains to manage environmental pollution and alleviate water scarcity, Nat. Hazards 110 (3) (2022) 2353–2380, https://doi.org/10.1007/s11069-021-05040-w.

[8] E. Ansari, N.L. Ferber, A.A. Hulleck, L.F. Dumée, N. Calvet, Performance of vapour compression based atmospheric water generation systems in arid conditions – Experimentations and perspectives in the Gulf region, J. Water Process Eng. (April) (2023), https://doi.org/10.1016/j.jwpe.2023.103739.

[9] A. Tripathi, S. Tushar, S. Pal, S. Lodh, S. Tiwari, P.R.S. Desai, Atmospheric water generator, Int. J. Enhanc. Res. Sci. Technol. Eng. 5 (4) (2016) 2319–7463.

[10] E. Ansari, et al., Atmospheric water generation in arid regions – a perspective on deployment challenges for the Middle East, J. Water Process Eng. 49 (2022), https://doi.org/10.1016/j.jwpe.2022.103163.

[11] A.A. Al-Farayedhi, N.I. Ibrahim, P. Gandhidasan, Condensate as a water source from vapor compression systems in hot and humid regions, Desalination 349 (2014) 60–67, https://doi.org/10.1016/j.desal.2014.05.002.

[12] A.J. Talib, A.H.N. Khalifa, A.Q. Mohammed, Performance study of water harvesting unit working under iraqi conditions, Int. J. Air-Conditioning Refrig. 27 (1) (2019), https://doi.org/10.1142/S2010132519500111.

[13] F. Faraz Ahmad, C. Ghenai, M. Al Bardan, M. Bourgon, A. Shanableh, Performance analysis of atmospheric water generator under hot and humid climate conditions, in: Drinkable Water Production and System Energy Consumption, vol. 6, Elsevier Ltd, 2022, https://doi.org/10.1016/j.cscee.2022.100270.

[14] O.A. Alduchov, R.E. Eskridge, Improved Magnus form approximation of saturation vapor pressure, J. Appl. Meteorol. Climatol. (1996) 601–609, https://doi.org/10.1175/1520-0450(1996)035%3C0601:IMFAOS%3E2.0.CO;2.

[15] K. Shi, Junjie Yang, Analysis and solution of condensation Phenomenon in ring main Unit, in: E3S Web of Conferences, 2021, https://doi.org/10.1051/e3sconf/202129003005.

[16] K. Uk, K. Kamal, D. Karunanidhi, Data analysis using box and whisker plot for functional point, in: International Conference on Trends in Electronics and Informatics, 2017.

[17] P.C. Banacos, Box and Whisker Plots for Local Climate Datasets: Interpretation and Creation Using Excel 2007/2010, 2011.

[18] G. Naga Raju, K. Dilip Kumar, T. Srinivasa Rao, Enhancement of cop of vapour compression refrigeration system by using diffusers, Int. J. Recent Technol. Eng. 8 (2) (2019) 6123–6129, https://doi.org/10.35940/ijrte.B3908.078219.

[19] P. F, et al., Incropera, *Fundamentals of Heat and Mass Transfer*, vol. 112, 2007, https://doi.org/10.1007/978-3-031-28920-0_19.

[20] L. Cattani, P. Cattani, A. Magrini, Air to water generator integrated system real application: a study case in a worker Village in United Arab Emirates, Appl. Sci. 13 (5) (2023), https://doi.org/10.3390/app13053094.

[21] N.A. Dahman, K.J. Al Juboori, E.A. Bukamal, F.M. Ali, K.K. Alsharooqi, S.A. Al-Banna, Water collection from air humidity in Bahrain, E3S Web Conf. 23 (2017) 1–15, https://doi.org/10.1051/e3sconf/20172303001.

[22] M. Aurangzaib, et al., Suitability of Atmospheric Water Harvesting (AWH) techniques for the climatic conditions of Pakistan : a case study 12 (3) (2023) 1490–1500.

[23] E. Ansari, N. Lopez, A. Aziz, L.F. Dum, Journal of Water Process Engineering Performance of vapour compression based atmospheric water generation systems in arid conditions – Experimentations and perspectives in the Gulf region 53 (January) (2023), https://doi.org/10.1016/j.jwpe.2023.103739.

[24] A.J. Talib, A.H.N. Khalifa, A.Q. Mohammed, Performance study of water harvesting Unit working under Iraqi conditions, Int. J. Air-Conditioning Refrig. 27 (1) (Mar. 2019) 1950011, https://doi.org/10.1142/S2010132519500111.

[25] F. Faraz Ahmad, C. Ghenai, M. Al Bardan, M. Bourgon, A. Shanableh, Performance analysis of atmospheric water generator under hot and humid climate conditions: drinkable water production and system energy consumption, Case Stud. Chem. Environ. Eng. 6 (Dec) (2022), https://doi.org/10.1016/j.cscee.2022.100270.

[26] J. Patel, K. Patel, A. Mudgal, H. Panchal, K.K. Sadasivuni, Experimental investigations of atmospheric water extraction device under different climatic conditions, Sustain. Energy Technol. Assessments 38 (Apr) (2020), https://doi.org/10.1016/j.seta.2020.100677.

[27] J. Kim, K. Park, D. Ryook, S. Hong, A comprehensive review of energy consumption of seawater reverse osmosis desalination plants, Appl. Energy 254 (April) (2019) 113652, https://doi.org/10.1016/j.apenergy.2019.113652.